Damage Detection in CFRP Laminates by Ultrasonic Wave Propagation Using MFC Actuator and FBG Sensor

Yoji Okabe and Fumihiro Nakayama

Department of Mechanical and Biofunctional Systems, Institute of Industrial Sciences, The University of Tokyo
4-6-1 Komaba, Meguro-ku, Tokyo 153-8505, Japan

For damage detection in CFRP laminates, health monitoring techniques using Lamb waves are effective. In this research, the authors constructed a new system combining a macro fiber composite (MFC) actuator and a fiber Bragg grating (FBG) sensor to employ broadband Lamb waves from DC to 1MHz. Then this system was applied to a CFRP quasi-isotropic laminate to examine the broadband characteristic. As a result, this system proved to be able to send and receive more broadband ultrasonic wave than conventional systems using bulk PZTs. Moreover, we investigated the frequency dispersion characteristic of Lamb waves propagating in the CFRP laminate in more detail by sending narrowband ultrasonic waves with different center frequencies. As a result, we could identify the modes of Lamb waves, comparing the measured frequency dispersion curves with the theoretical dispersion curves. After that, the dispersion curves were measured for the CFRP laminate that included an artificial delamination. Since the result measured in the damaged laminate had different dispersion from the result in the intact laminate, the delamination could be detected from the frequency dispersion curves. Hence this system can obtain more effective information for damage detection.

Key Words: Lamb Wave, FBG Sensor, MFC Actuator, CFRP Laminate, Broadband Characteristic

1. Introduction

In Recent years, CFRP composite laminates have been applied to lightweight structures, such as space structures and aircrafts. However, since CFRP laminates have complex fracture process, structural health monitoring systems are attracting attention. The systems use sensors pre-installed into composite members and diagnose the structural health easily in real time. As one of the techniques, Lamb waves propagating along the laminates are used for the diagnosis [1]. Damages in the laminates can be detected from the change in the received waves. In general, bulk piezo-electric ceramics (PZTs) are used to send and receive the ultrasonic waves. In that case, since the bulk PZTs have the resonant frequency, the generated ultrasonic waves are limited within the narrowband.

However, the authors have succeeded in receiving ultrasonic waves by using fiber Bragg grating (FBG) sensors that are a kind of optical fiber sensors [2-3]. Moreover, macro fiber composite (MFC) actuators [4] developed in NASA consist of a lot of thin PZT fibers embedded into epoxy resin and can be used as a generator of ultrasonic waves. These components do not have the resonant frequency and have directional sensitivity because both of them are fibrous. Thus broadband ultrasonic waves can be sent and received efficiently in a specific direction by the combination of these components. Therefore, when a time-frequency analysis is applied to the received waves, more information will be obtained compared with the measurement with a wave of only single frequency. Then, when the relation between the damage size in the propagation path and the change in frequency components is clarified, the damage diagnosis is expected to improve its accuracy.

In this research, the authors constructed a system consisting of an MFC actuator to generate broadband Lamb waves and an FBG sensor to receive the propagated waves. Then this system was applied to a CFRP quasi-isotropic laminate to examine the broadband characteristic, compared with the conventional systems using bulk PZTs. Moreover, we investigated the frequency dispersion characteristic of Lamb waves in the CFRP laminate by sending narrowband ultrasonic waves with different center frequencies. Then the dispersion curves measured for the intact laminate and that for the damaged laminate were compared in order to investigate the capability of damage detection.

2. System Configuration

The MFC actuator used to excite broadband waves is a flexible actuator developed in NASA Langley Research Center and commercialized in Smart Material Corp. The MFC consists of rectangular PZT fibers sandwiched between layers of epoxy adhesive and polyimide film with interdigitated electrodes. Large strain can be generated in one direction by the MFC with the d33 effect. The dimensions of the MFC actuator used in this research are 6mm in the longitudinal length and 13.5mm in the width.

The FBG sensor used to receive propagated waves is a kind of optical fiber sensors. The FBG is fabricated in an optical fiber to have a periodic variation in the refractive index along a certain length of the core. When a broadband light is injected into the core, the FBG reflects a narrow spectral component at the Bragg wavelength that is proportional to the applied strain. Recently, the authors developed a high-speed optical wavelength interrogation system in cooperation with Hitachi Cable Ltd. This system uses an AWG filter to sense the Bragg wavelength and can detect high-speed strain changes caused by the propagation of ultrasonic waves. The FBG used in this research is a small-diameter FBG sensor with the gauge length of 1.5mm and coated with polyimide whose outside diameter is 60μm (Hitachi Cable Ltd.).

The MFC excites the normal strain axially in the PZT fibers and FBG detects the axial strain in the fibrous optical fiber. Hence these elements have a broadband response because of no resonant frequency and have a strong directional sensitivity compared with bulk PZTs. First, the MFC actuator and the FBG sensor are bonded on the CFRP laminate as shown in Fig. 1. Then, a waveform signal generated with a multifunction generator (WF1974, NF Corporation) is amplified to a high-voltage signal by a high-speed bipolar amplifier (HSA4012, NF Corporation) and input to the MFC for excitation of ultrasonic waves. After that, the wave propagated in the structure reaches the FBG sensor, and the strain change is converted into the voltage signal by the high-speed optical wavelength interrogation system and displayed on a digital oscilloscope (DL708E, YOKOGAWA).

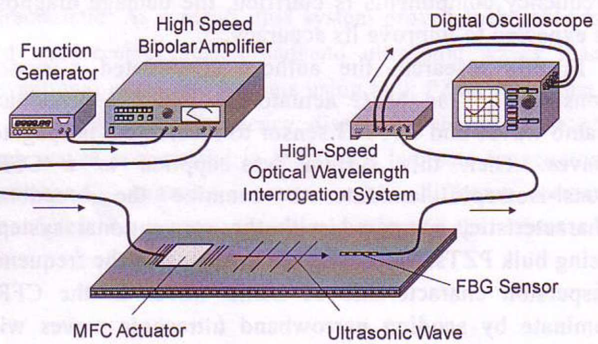

Fig. 1. Propagation system of broadband ultrasonic waves using MFC and FBG.

3. Confirmation of the Broadband Characteristic

In order to confirm the performance of this system, a broadband Lamb wave was propagated in a CFRP quasi-isotropic laminate of 3mm in the thickness (T700S/2500, $[45/0/-45/90]_{3s}$, Toray Industries, Inc.). The MFC actuator and the FBG sensor were separated by 40mm and were bonded on the surface of the laminate with a cyanoacrylate adhesive. The voltage signal input to the MFC is one-cycle sinusoidal wave at 250kHz with Hamming window. The input waveform is plotted in Fig. 2 with the Fourier transform result. This input wave is confirmed to be broadband from DC to about 600kHz. In the measurement, 32768 received waves were averaged for noise reduction. For comparison, we also propagated Lamb waves using two types of AE sensors consisting of bulk PZTs: a resonance-model AE sensor with the resonant frequency of 350kHz (M31, Fuji Ceramics Corp., the diameter: 3mm) and a wide-bandwidth AE sensor with the frequency range of 200kHz to 1300kHz (1045S, Fuji Ceramics Corp., the diameter: 20mm). In this paper, the case with the MFC actuator and the FBG sensor is called MFC-FBG for short, the case with the resonance-model AE sensors used for a transmitter and a receiver is called Resonant PZT-PZT, and the case with the wide-bandwidth AE sensors for a transmitter and a receiver is called Broadband PZT-PZT.

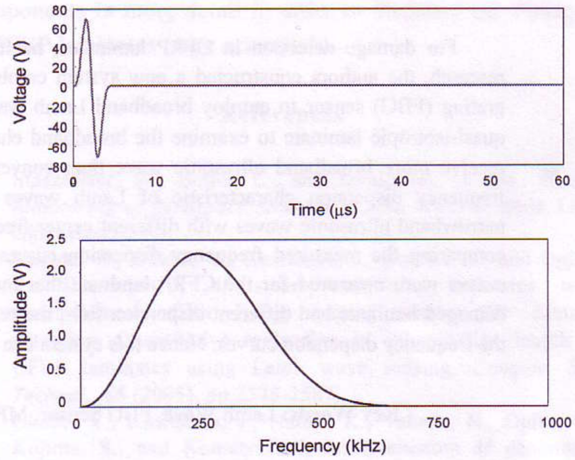

Fig. 2. Broadband input waveform and the Fourier transform result.

The received waveform, the Fourier transform result, and the wavelet transform result in the case of the MFC-FBG are shown in Fig. 3, and those in the cases of the Resonant PZT-PZT and the Broadband PZT-PZT are plotted in Figs. 4 and 5, respectively. The complex Morlet wavelet was used for the wavelet transform. In the result of the Fourier transform for the Resonant PZT-PZT, one sharp peak appears at about 300kHz due to the resonant frequency of 350kHz. Even the result of the Broadband PZT-PZT has a major peak at about 220kHz. On the other hand, the Fourier transform result in the MFC-FBG shows broadband frequency components. Hence the wavelet transform result in the MFC-FBG reflects the frequency dispersion of the Lamb waves more clearly than that of the Resonant PZT-PZT and that of the Broadband PZT-PZT. These results indicate that the MFC-FBG has the better broadband characteristic since both the MFC and the FBG do not have the resonant frequency.

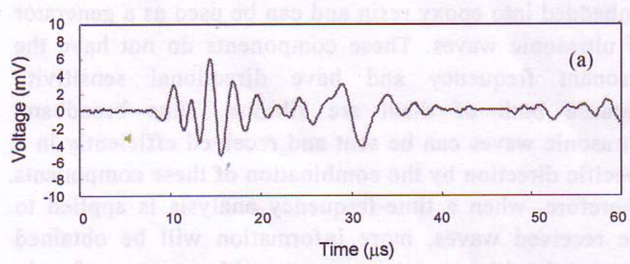

Fig. 3. Results in the MFC-FBG: (a) received wave, (b) Fourier transform result, and (c) wavelet transform result.

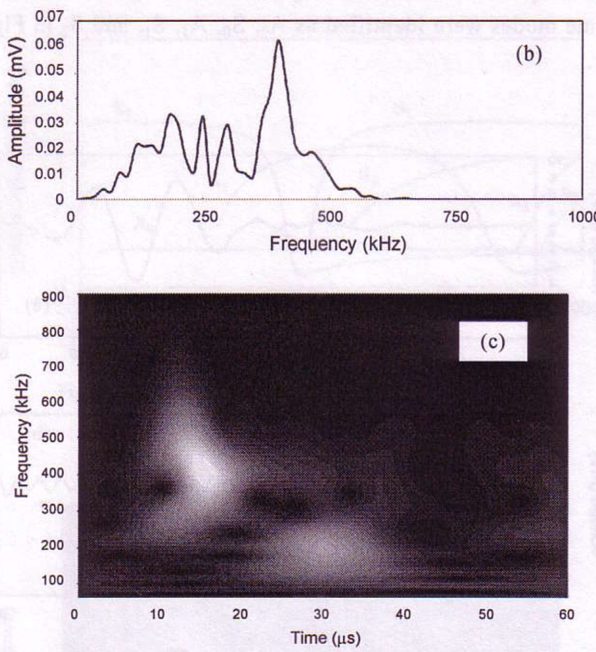

Fig. 3(Continued). Results in the MFC-FBG: (a) received wave, (b) Fourier transform result, and (c) wavelet transform result.

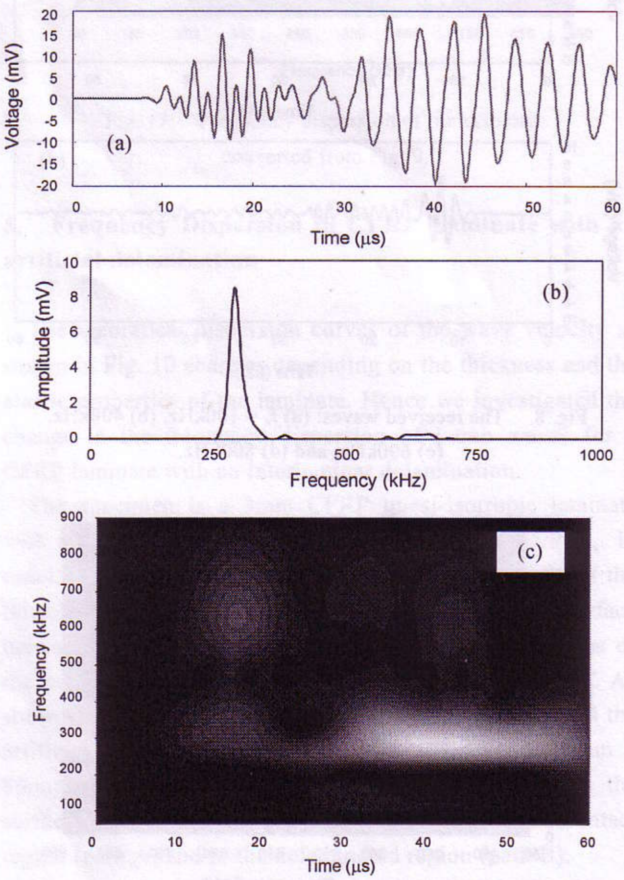

Fig. 4. Results in the Resonant PZT-PZT: (a) received wave, (b) Fourier transform result, and (c) wavelet transform result.

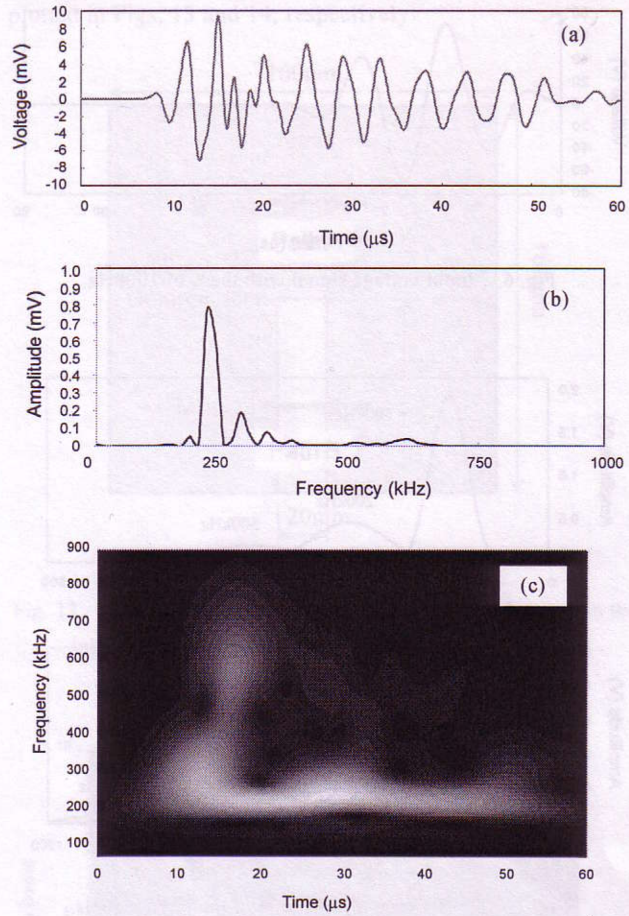

Fig. 5. Results in the Broadband PZT-PZT: (a) received wave, (b) Fourier transform result, and (c) wavelet transform result.

4. Frequency Dispersion of Lamb Waves in CFRP Laminate

In the wavelet transform result obtained by this system (Fig. 3(c)), the mode dispersion of the Lamb waves was able to be found. This frequency dispersion characteristic will be a useful information for damage identification because the wavelength of Lamb waves highly relates to the length of the damage in the propagation direction. Hence the authors investigated the mode dispersion characteristic of Lamb waves propagating in the CFRP laminate in more detail by sending narrowband ultrasonic waves with different center frequencies.

The input waveform was three-cycle sinusoidal waves at the frequency f_c with Hamming window. The center frequency f_c was changed from 100kHz to 900kHz at 100kHz intervals. As an example, the input voltage signal with the f_c of 100kHz is shown in Fig. 6. Also, the Fourier transform results of the input signals are plotted in Fig. 7. With an increase in the center frequency f_c, the spectrum broadened and the highest peak decreased, since the duration of the input wave became shorter.

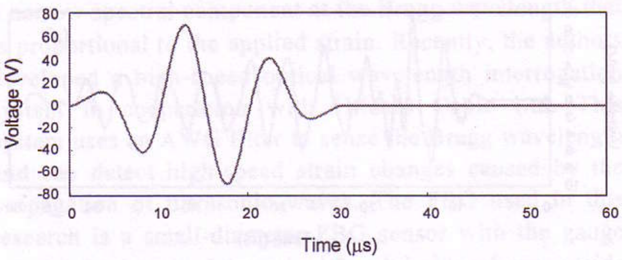

Fig. 6. Input voltage signal with the f_c of 100kHz.

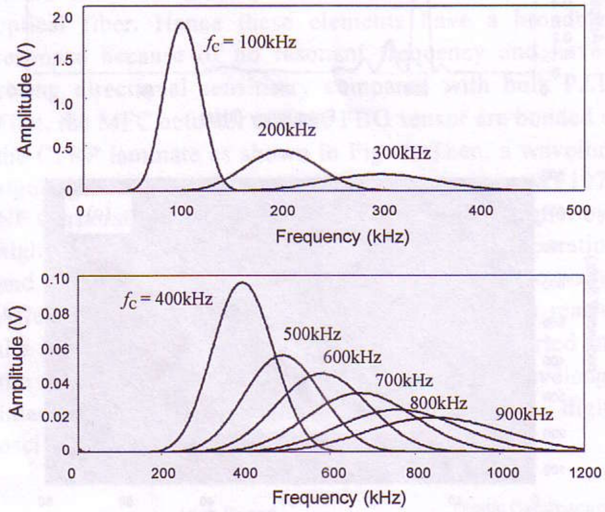

Fig. 7. Fourier transform results of the input signals.

These voltage signals were input into the MFC actuator and the propagated waves were received in the FBG sensor. Although the amplitude of the received wave became small in the higher frequency range, the propagated Lamb waves were observed at all the center frequency f_c as shown in Fig. 8. For the measured waveforms, the wavelet transform was applied. Then the absolute values of the complex wavelet coefficients were calculated in the frequency range from f_c - 50kHz to f_c + 50kHz, and the absolute values were normalized by the largest component at each frequency. After that, all the normalized modulus of the wavelet coefficients were plotted in Fig. 9 from 50kHz (f_c = 100kHz) to 950kHz (f_c = 900kHz). Some modes of Lamb waves were observed in this graph. Hence group velocities of Lamb waves in the CFRP quasi-isotropic laminate were calculated theoretically [5] and plotted in Fig. 10. In order to compare the experimental result shown in Fig. 9 to the theoretical dispersion curves in Fig. 10, the vertical axis of the arrival time in Fig. 9 was converted into the velocity for the propagation length of 40mm and the result was redrawn in Fig. 11. Compared with Fig. 10, the group velocities of the modes appearing in Fig. 11 are slightly smaller. This is because the arrival time in Fig. 9 was determined from the origin fixed to the rising edge of the input wave, so that the actual arrival time of the wave energy was shorter. Through the comparison between the Fig. 11 and the Fig. 10, however, some modes were identified as A_0, S_0, A_1, S_1, and S_2 in Fig. 11.

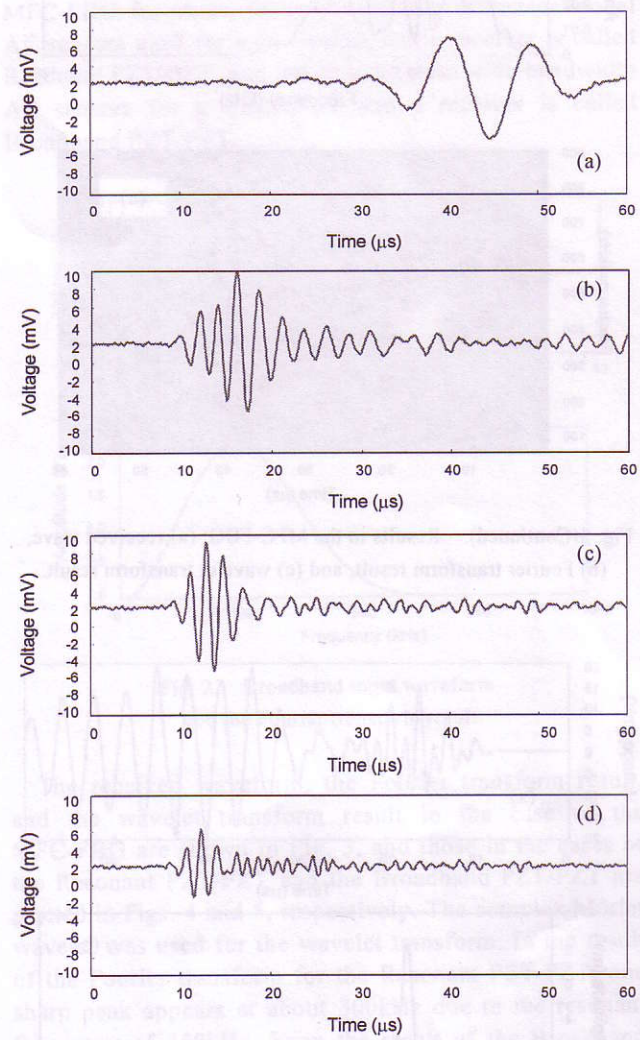

Fig. 8. The received waves: (a) f_c = 100kHz, (b) 400kHz, (c) 600kHz, and (d) 800kHz.

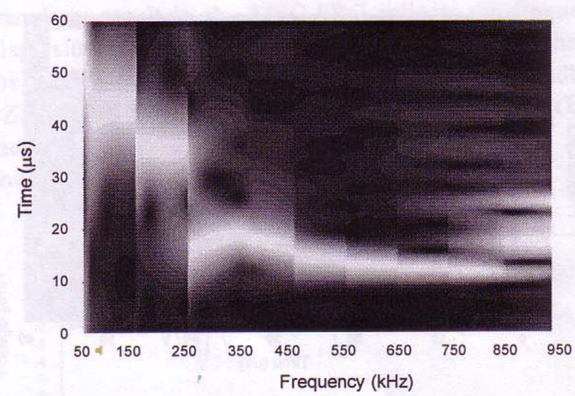

Fig. 9. Normalized modulus of wavelet coefficients obtained from all the measured waves.

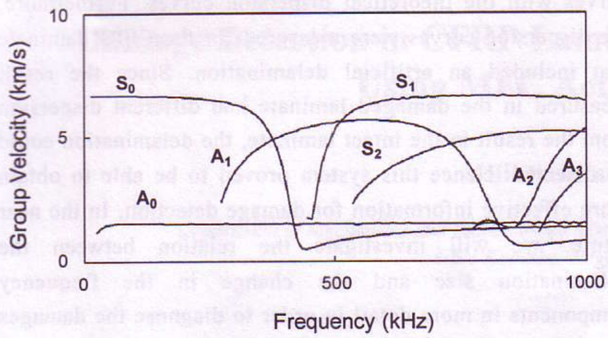

Fig. 10. Theoretical group velocities of Lamb waves propagating in the CFRP laminate.

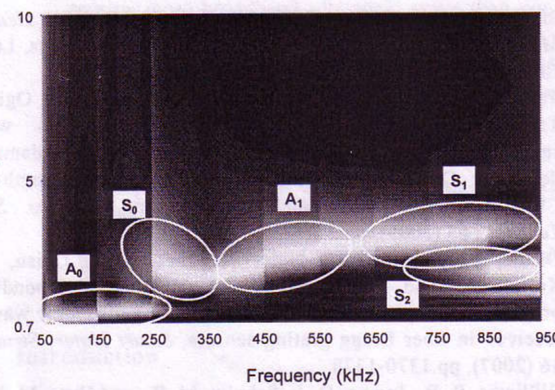

Fig. 11. Frequency dispersion of the velocity converted from Fig. 9.

5. Frequency Dispersion in CFRP Laminate with an artificial delamination

The theoretical dispersion curves of the wave velocity as shown in Fig. 10 changes depending on the thickness and the elastic properties of the laminate. Hence we investigated the change in the frequency dispersion of Lamb waves for a CFRP laminate with an interlaminar delamination.

The specimen is a 3mm CFRP quasi-isotropic laminate with the same laminate configuration of $[45/0/-45/90]_{3s}$. In order to form an artificial delamination in the middle of the thickness, a 50μm Teflon film was embedded in the interface between two 90° plies during the manufacturing process of the laminate, and the film was removed after the curing. As shown in Fig. 12, the dimensions of the laminate and the artificial delamination were 160mm × 160mm and 20mm × 80mm. Two pairs of MFC and FBG were bonded on the surface of the laminate to propagate Lamb waves in the intact region (path A) and in the delaminated region (path B).

In the same way as the experiment described in the chapter 4, the narrowband ultrasonic waves from 100kHz to 900kHz were propagated, and the wavelet transform results of the received waves were normalized. The frequency dispersion of the velocity obtained in the path A and the path B are plotted in Figs. 13 and 14, respectively.

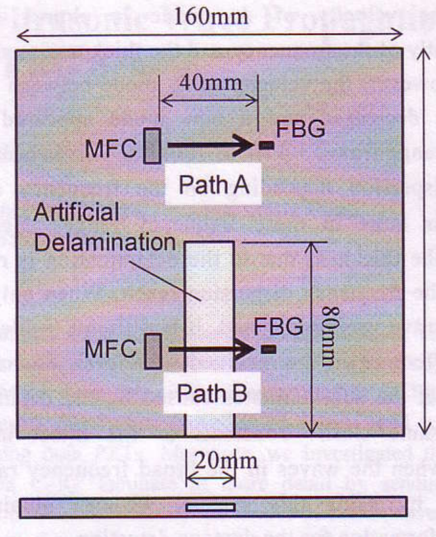

Fig. 12. Experimental setup for propagation of Lamb waves in the intact region (path A) and the damaged region (path B) using MFC and FBG.

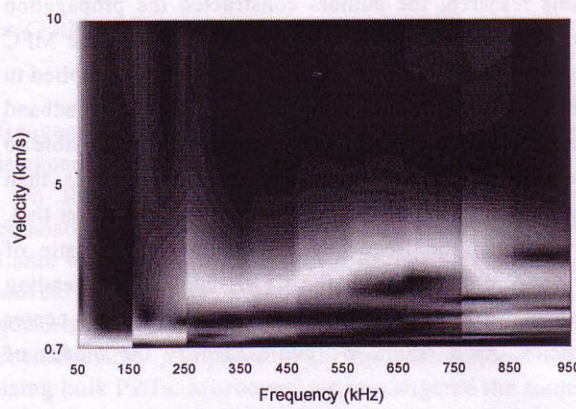

Fig. 13. Frequency dispersion obtained in the path A.

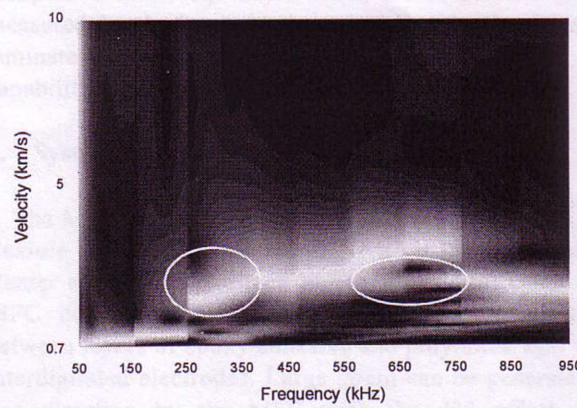

Fig. 14. Frequency dispersion obtained in the path B.

The frequency dispersion curves measured in the path A (Fig. 13) is almost the same as the former result shown in Fig. 11. This agreement shows that this measurement system has high reproducibility. On the other hand, the result measured in the path B is slightly different from that in the path A. The A_0 mode under the frequency of 250kHz did not change, because the velocity of A_0 mode is almost constant independently of the frequency and the thickness as shown in Fig. 10. However, the velocity of S_0 mode between 250kHz to 350kHz decreased and a new mode appeared in the frequency range from 550kHz to 750kHz. This is because the velocity dispersion depending on the frequency and the thickness is large in these frequency ranges. Hence the change in the thickness due to the delamination is reflected clearly in the frequency dispersion result. When only single frequency wave was propagated, it is difficult to identify an obvious difference in the received waveform, especially, in the case that the sub-laminates caused by the delamination have the same elastic constants as the intact laminate. However, when the waves in the broad frequency range are propagated by using this system, we can obtain more effective information for the damage detection.

6. Conclusions

In this research, the authors constructed the propagation system of broadband ultrasonic waves combining the MFC actuator and the FBG sensor. Then the system was applied to the CFRP quasi-isotropic laminate to examine the broadband characteristic. As a result, this system proved to be able to send and receive more broadband ultrasonic waves than conventional ultrasonic systems using bulk PZTs. After that, we investigated the frequency dispersion characteristic of Lamb waves propagating in the CFRP laminate by sending narrowband ultrasonic waves with different center frequencies. As a result, we could identify the modes of Lamb waves, comparing the measured frequency dispersion curves with the theoretical dispersion curves. Furthermore, the dispersion curves were measured for the CFRP laminate that included an artificial delamination. Since the result measured in the damaged laminate had different dispersion from the result in the intact laminate, the delamination could be detected. Hence this system proved to be able to obtain more effective information for damage detection. In the near future, we will investigate the relation between the delamination size and the change in the frequency components in more detail in order to diagnose the damages in CFRP laminates more accurately.

References

1) Staszewski, W., Boller, C., and Tomlinson, G. eds.: *Health Monitoring of Aerospace Structures*, John Wiley & Sons, Ltd., Chichester, 2004.
2) Takeda, N., Okabe, Y., Kuwahara, J., Kojima, S., and Ogisu, T.: Development of smart composite structures with small-diameter fiber Bragg grating sensors for damage detection: Quantitative evaluation of delamination length in CFRP laminates using Lamb wave sensing, *Compos. Sci. Technol.*, **65** (2005), pp.2575-2587.
3) Okabe, Y., Kuwahara, J., Natori, K., Takeda, N., Ogisu, T., Kojima, S., and Komatsuzaki, S.: Evaluation of debonding progress in composite bonded structures using ultrasonic waves received in fiber Bragg grating sensors, *Smart Mater. Struct.*, **16** (2007), pp.1370-1378.
4) Williams, R. B., Inman, D. J., Schultz, M. R., and Hyer, M. W., Nonlinear tensile and shear behavior of macro fiber composite actuators, *J. Compos. Mater.*, **38** (2004), pp.855-869.
5) Nayfeh, A. H., *Wave Propagation in Layered Anisotropic Media*, Elsevier, Amsterdam, 1995.